Received: 5 November 2020 | Accepted: 19 January 2022

DOI: 10.1111/poms.13691

POMS

ORIGINAL ARTICLE

A new perspective on breast cancer diagnostic guidelines to reduce overdiagnosis

Sait Tunç[1] | **Oguzhan Alagoz**[2] | **Elizabeth S. Burnside**[3]

[1]Grado Department of Industrial and Systems Engineering, Virginia Tech, Blacksburg, Virginia, USA

[2]Department of Industrial and Systems Engineering, University of Wisconsin-Madison, Madison, Wisconsin, USA

[3]Department of Radiology, University of Wisconsin-Madison, Madison, Wisconsin, USA

Correspondence
Sait Tunç, Grado Department of Industrial and Systems Engineering, Virginia Tech, Blacksburg, VA 24061, USA.
Email: sait.tunc@vt.edu

Funding information
National Cancer Institute, Grant/Award Numbers: K24CA194251, P30CA014520, R01CA165229

Handling editor: Sergei Savin

Abstract

Overdiagnosis of breast cancer, defined as diagnosing a cancer that would otherwise not cause symptoms or death in a patient's lifetime, costs U.S. health care system over $1.2 billion annually. Overdiagnosis rates, estimated to be around 10%–40%, may be reduced if indolent breast findings can be identified and followed with noninvasive imaging rather than biopsy. However, there are no validated guidelines for radiologists to decide when to choose imaging options recognizing cancer grades and types. The aim of this study is to optimize breast cancer diagnostic decisions based on cancer types using a large-scale finite-horizon Markov decision process (MDP) model with 4.6 million states to help reduce overdiagnosis. We prove the optimality of a divide-and-search algorithm that relies on tight upper bounds on the optimal decision thresholds to find an exact optimal solution. We project the high-dimensional MDP onto two lower dimensional MDPs and obtain feasible upper bounds on the optimal decision thresholds. We use real data from two private mammography databases and demonstrate our model performance through a previously validated simulation model that has been used by the policy makers to set the national screening guidelines in the United States. We find that a decision-analytical framework optimizing diagnostic decisions while accounting for breast cancer types has a strong potential to improve the quality of life and alleviate the immense costs of overdiagnosis. Our model leads to a 20% reduction in overdiagnosis on the screening population, which translates into an annual savings of approximately $300 million for the U.S. health care system.

KEYWORDS
breast cancer, diagnostic decisions, large-scale dynamic programming, Markov decision processes, overdiagnosis

1 | INTRODUCTION

Breast cancer is the most common nonskin cancer affecting women in the United States. Approximately one in every eight American women is expected to develop invasive breast cancer during their lifetime, and one in every 36 American women is expected to die from this disease. An effective way to reduce breast cancer mortality is early diagnosis through screening mammography (Khatib & Modjtabai, 2006). Although there is a controversy on the starting age and the frequency of mammography screening, many medical organizations such as The American College of Obstetricians and Gynecologists (ACOG) recommend annual screening mammography beginning at age 40 (ACOG, 2020).

Using a mammography exam, radiologists identify findings, categorize these findings with descriptors, and render a recommendation based on an estimate of the probability of cancer. There are three main postmammographic diagnostic options for radiologists:

(i) additional imaging and biopsy,
(ii) short-term follow-up mammography in 6 months, or
(iii) routine follow-up mammography in a year.

Accepted by Sergei Savin, after 1 revision.

Surprisingly, there are only a few validated quantitative guidelines for radiologists to decide which option to choose after a mammography exam.

Although screening mammography saves thousands of lives every year through early diagnosis, it has several harms including a large number of false positives and overdiagnosis. In particular, overdiagnosis of breast cancer, defined as diagnosing a condition that would otherwise not cause symptoms or death in a patient's lifetime, has been the focus of many recent studies in the breast cancer literature over the last decade (Srivastava et al., 2019) and received extensive media coverage (CNN, 2018; Medscape, 2020; New York Times, 2017; Washington Post, 2017). The proportion of breast cancer cases that were overdiagnosed has been estimated to be between 10% and 40% (Bleyer & Welch, 2012; Duffy et al., 2005; Jørgensen et al., 2017; Miller et al., 2014). In 2012, scientists from diverse disciplines gathered at National Cancer Institute's (NCI) meeting on overdiagnosis to evaluate the problem of cancer overdiagnosis and acknowledged the necessity of new screening and diagnostic guidelines to lessen overdiagnosis (Esserman et al., 2013). A recent study further revealed that breast cancer overdiagnosis costs the U.S. health care system over $1.2 billion every year (Ong & Mandl, 2015).

A major cause of overdiagnosis is diagnosing indolent tumors, which either never progress or progress so slowly that the patient dies of other causes before the tumor produces symptoms (Welch & Black, 2010). Several autopsy studies report such findings in patients who die before cancer becomes symptomatic (Esserman et al., 2013). However, current diagnostic guidelines do not consider the differential risk of developing indolent and aggressive tumors. In the current clinical practice, a scalar risk corresponding to the cumulative risk of breast cancer is used for making the diagnostic decisions, where findings with more than 2% probability of cancer are recommended biopsy regardless of the age of the woman (BI-RADS, 2003). There have been encouraging findings in the cancer genomics literature showing that gene expression signatures may predict indolent or aggressive cancer (Esserman et al., 2017; Irshad et al., 2013), yet no previous study in the medical and operational literature that aimed to improve the current clinical guidelines has considered tailoring diagnostic decisions based on the risk of developing different cancer types (see Section 2). Can neglecting the age-specific differences between indolent and aggressive cancers in making diagnostic decisions contribute to the alarming rates of overdiagnosis? Our main aim in this paper is to affirmatively answer this question through proposing an alternative perspective on breast cancer diagnosis that requires a two-step modeling approach. The first step is to estimate a multidimensional breast cancer risk vector, which encompasses the risk of aggressive and indolent types of cancers and use it for decision making instead of a scalar risk representing the cumulative probability of cancer risk. Using such a multidimensional risk vector enables special care for indolent diseases, which are more likely to be overdiagnosed compared to more aggressive diseases. And the second step is to provide novel optimization algorithms to overcome the computational challenges that inevitably arise with the use of multidimensional risk estimates for diagnostic decision making, a phenomenon known as the *curse of dimensionality*.

The purpose of this paper is therefore to determine the optimal breast cancer diagnostic decisions with a practically pertinent setup tailored to the type of cancer and to evaluate its effect on reducing overdiagnosis, based on a woman's age. Our goal is to offer a remedy for overdiagnosis through a multidimensional optimization of breast cancer diagnostic decisions based on disease types and consequently skipping aggressive diagnostic procedures on patients who do not need them. To determine whether a patient needs an invasive postmammogram procedure, we use quality-adjusted life years (QALYs) to measure her health gain from such procedures. Our approach offers a potent solution to the lack of a comprehensive optimization tool to guide radiologists in making decisions that integrate indolent and aggressive types of breast cancer and thus eliminates a major cause of overdiagnosis. We develop a large-scale Markov decision process (MDP) model to find the optimal postmammography diagnostic actions based on mammographic descriptors and demographic factors to maximize the total expected health benefits measured by QALYs. Using a multidimensional risk model contributes to the existing models in the literature that use a simplified scalar risk, ignoring the substantial differences among breast cancer types. We derive the structural properties of the optimal diagnostic policies to develop easy-to-implement and efficient algorithms to find an exact optimal solution for the otherwise computationally intractable MDP.

Among various breast cancers, a prevalent and well-studied indolent type is ductal carcinoma in situ (DCIS), which is defined as the presence of abnormal cells inside the milk ducts that have not spread outside the ducts. Between 1975 and 2004, the age-adjusted incidence rate of DCIS increased from 1.87 to 32.7 per 100,000 women-years (Virnig et al., 2009). DCIS is categorized into three types with respect to tumor growth rate: low-, intermediate-, and high-grade (Allred, 2010). While DCIS is not life-threatening, the current clinical practice is to diagnose and treat all DCIS cases because DCIS can progress to invasive breast cancer (Fisher et al., 2001). However, DCIS may remain indolent for several years and not progress to invasive cancer in a woman's lifetime. Furthermore, DCIS sojourn time, defined as the mean duration of the preclinical phase, depends on its grade, with high-grade DCIS progressing to invasive cancer faster than low-grade. As a result of the substantial differences among the progression rates of different DCIS grades, experts suggest that mammography findings that may indicate low-grade DCIS may be followed with noninvasive imaging rather than biopsy in older women (van Luijt et al., 2016). We analytically investigate the effects of this hypothesis by incorporating the grade of DCIS, which captures the heterogeneity of DCIS tumors concerning their potential for leading to cancer death, into our model.

Our contributions in this paper can be summarized as follows. First, we provide patient-specific optimal diagnostic thresholds by assessing a multifaceted risk vector for each

woman using mammographic findings. We then evaluate the effect of the optimal diagnostic policies obtained by our model on reducing breast cancer overdiagnosis based on the patient's age. Furthermore, rather than solving an approximate dynamic programming, we develop an efficient and easily implementable divide-and -search (DS) algorithm to find the exact solution to the given large-scale MDP in polynomial time. We also provide a projection method from the high-dimensional MDP into lower dimensional MDPs to introduce feasible upper bounds on the diagnostic thresholds by utilizing the analytical characteristics of the breast cancer decision-making problem. The proposed dimension reduction method supplements the solution algorithm by providing limits on the necessary parameters to be calculated and stored. We optimally solve the MDP model using clinical data from two established hospitals and demonstrate our model performance through a previously validated simulation model that has been used by the policymakers to set the national screening guidelines in the United States. Our results show that the optimal diagnostic guidelines provided by our model lead to a significant reduction in overdiagnosis, where the rate of reduction increases with age. While the current form of the solution algorithm and the dimension reduction method is tailored for breast cancer diagnostic decisions, our framework has the potential for use in other medical decision-making problems that involve a variety of disease types.

The remainder of this paper is organized as follows. Relevant literature is surveyed in Section 2. A large-scale MDP model to optimize the breast cancer diagnostic decisions is presented in Section 3. The structural properties of the optimal policy are derived in Section 4. An efficient algorithm to exactly solve the given large-scale MDP is developed in Section 4.1. A reduced dimension model to provide feasible bounds on the optimal diagnostic thresholds found by the solution algorithm is presented in Section 4.2. In Section 5, we describe the estimation of model parameters that are used to conduct the numerical experiments given in Section 6. Finally, concluding remarks and future extensions are presented in Section 7.

2 | LITERATURE REVIEW

The operations research literature on the optimization of breast cancer policies focuses on two different aspects of the problem: screening and diagnosis. On the screening side, several models have been proposed either from a population-based perspective (Cevik et al., 2018; Maillart et al., 2008) or from a personalized perspective (Ayer et al., 2012, 2015). On the diagnostic side, Chhatwal et al. (2010) propose a finite-horizon discrete-time MDP model to determine the optimal biopsy threshold based on a scalar risk of cancer. Alagoz et al. (2013) provide an extension by including the short-term follow-up as a diagnostic action to improve clinical relevance. Ayvaci et al. (2012) consider diagnostic decisions under budgetary constraints and develop a mixed-integer programming formulation to optimally solve the corresponding constrained MDP model. Contrasted with our work, these papers use a scalar probability of cancer and make policy recommendations without discriminating whether the findings indicate an indolent or aggressive cancer. Furthermore, as a result of the lack of a multidimensional risk model, they ignore the heterogeneity of cancer types with respect to their rate of progression and potential for leading to cancer death.

The problem of overdiagnosis and overtreatment has been considered in various settings. A major stream in the literature focuses on reporting overdiagnosis rates through prospective cohort studies or follow-ups of randomized controlled trials that compare the incidence among an intervened population to a reference population (Bleyer & Welch, 2012; Duffy et al., 2005; Jørgensen et al., 2017; Miller et al., 2014). A few other studies propose analytical frameworks to quantify overdiagnosis or overtreatment. Paç and Veeraraghavan (2015) study the overtreatment problem using a queuing game approach, and conclude that experts may tend to overtreat their customers by exploiting their informational advantage over them unless such a tendency is not weakened by congestion. In our setting, information asymmetry is not a concern. Arrospide et al. (2015) use discrete event simulation to assess the effectiveness of the Basque Country screening program using several measures including overdiagnosis in Basque women. Gunsoy et al. (2014) develop a Markov simulation model to evaluate the effects of different screening strategies on overdiagnosis and mortality using a cohort of British women. Madadi et al. (2018) propose a mixed-integer linear model to obtain screening policies that minimize a linearized function of breast cancer overdiagnosis and mortality. Seigneurin et al. (2011) perform approximate Bayesian computation analysis with a stochastic simulation model to quantify overdiagnosis by screening mammography in a cohort of French women. Davidov and Zelen (2004) present a mathematical framework to derive the probability of overdiagnosis and apply this framework to hypothetical early detection programs for prostate cancer.

The main differences between our work and the relevant literature on overdiagnosis are that they:

(i) do not consider all breast cancer types and the resulting heterogeneity in the progression of the disease,
(ii) ignore sequential decision making that is observed in diagnostic decisions, and
(iii) do not evaluate age-specific decisions based on patients' risk of cancer.

Compared to the literature, we implement a medically accurate model of the progression for each disease type and design a comprehensive decision-making scheme optimizing age-specific diagnostic decisions by concomitantly integrating the risks of indolent and aggressive types. Accordingly, we can establish the optimal policies that improve the early diagnosis of aggressive diseases while minimizing unnecessary procedures on low-risk diseases, which would not be possible using traditional approaches.

This paper further contributes to the growing literature on sequential decision making using a multidimensional risk vector to discriminate types of outcomes. Although including a high-dimensional risk vector enhances the rationality of the model, it also increases the size of the problem and makes MDPs harder to solve due to the curse of dimensionality (Puterman, 1994). Therefore, the use of multidimensional system states in sequential decision making is mostly limited to the areas of applications such as machine maintenance (Eckles, 1968; Helm et al., 2015; Makis, 2008), where, unlike the problem of interest, the total number of states is not very large to make the problem intractable to provide an exact solution.

3 | MODEL FORMULATION

We formulate the breast cancer diagnostic decision problem as a discrete-time, finite-horizon, large-scale MDP model and refer to it as the large-scale diagnostic decision model (LSM). We assume that the decision maker is the radiologist who is acting on behalf of the patient and the patient follows the recommendations of the radiologist. Diagnostic decisions are assumed to be made at discrete points $t = 0, 1, 2, \dots, T$, $T < \infty$, where t is defined as the number of 6-month intervals between the age of 40 and 100 (Arias, 2015). After a routine annual mammogram, the patient's risks of low-, intermediate-, high-grade DCIS and invasive cancer are estimated by the radiologist using one of the methods described in Section 5. Here, the grade of DCIS refers to its *cytologic grade*, which is classified by pathologists into three categories: grade 1 or "low-grade," grade 2 or "intermediate-grade," and grade 3 or "high-grade"(Allred, 2010). We define the system state using a cancer risk vector at time t as $x_t \in \bar{\mathcal{X}} \cup \{PT, D\}$. Here, PT represents the posttreatment state, D represents the death state, and $\bar{\mathcal{X}}$ is the set of risk vectors $x = [x^0, x^1, x^2, x^3, x^4]$ such that $x^i \in \{0, 1, \dots, 100\}$ for $i = 0, 1, 2, 3, 4$ and $\sum_{i=0}^{4} x^i = 100$[1]. The risk vectors $x \in \bar{\mathcal{X}}$ are breast cancer probability vectors such that x^0, x^1, x^2, x^3, and x^4 represent the probabilities of being cancer-free, low-grade DCIS, intermediate-grade DCIS, high-grade DCIS, and invasive cancer, respectively. The risk vectors are discretized for notational clarity. For example, if the probability of being cancer-free is 50%, low-grade DCIS is 20%, intermediate-grade DCIS is 15%, high-grade DCIS is 10%, and invasive cancer is 5%, then the corresponding risk vector is $[50, 20, 15, 10, 5]$.

Based on the risk vector (5-tuple), the radiologist may recommend: (i) immediate biopsy, (ii) short-term follow-up with a mammogram in 6 months, and (iii) routine follow-up with a mammogram in a year. If the radiologist recommends a biopsy and the biopsy confirms DCIS or invasive cancer, the patient moves to the posttreatment state, immediately starts receiving treatment, and the decision process ends. If the biopsy outcome is negative (benign) or the woman is recommended to have a short-term or routine follow-up, she stays in the decision process until the next corresponding decision epoch unless she dies at any point during that time interval. Therefore, the decision process ends either when the patient develops breast cancer or dies. Accordingly, we define the action space for a patient in state $x \in \bar{\mathcal{X}}$ as $A_x = \{\text{Short-term follow-up(Sf), Annual mammogram(Am), Biopsy(Bx)}\}$. When the patient is in state PT or D, the decision problem ends and there is no action associated with these states. Figure 1 depicts the decision process of the LSM.

Patients' risk of developing breast cancer types stochastically evolves throughout the decision process. Let $p_t(j|x, a)$ represent the probability that the patient will be in state j at time $t + 1$, given that the patient is in state x and the action is $a \in \mathcal{A}_x$ at time t. We define $p_t(PT|PT, a) = p_t(D|D, a) = 1$ for every $a \in \mathcal{A}$ and $t = 1, \dots, T$, since the posttreatment and death states are absorbing. We assume that the patient is not allowed to move to the posttreatment state without having a biopsy, hence we define $p_t(PT|x, a) = 0$ for $a \in \{\text{Sf}, \text{Am}\}$ and $x \in \bar{\mathcal{X}}$.

We define an equivalent state space to $\bar{\mathcal{X}}$, denoted by $\mathcal{X}$, such that for any $x \in \mathcal{X}$, $x = [x^1, x^2, x^3, x^4]$, where $0 \le x^1, x^2, x^3, x^4$ and $\sum_{i=1}^{4} x_t^i \le 100$.[2] Definition 1 provides the marginal probabilities of outcomes corresponding to each state $x_t \in \mathcal{X}$.

Definition 1. For any $x \in \mathcal{X}$, $\rho^i(x)$ denotes the probability of being cancer-free, low-grade DCIS, intermediate-grade DCIS, high-grade DCIS, and invasive cancer, for $i = 0, 1, 2, 3, 4$, respectively, that is, $\rho^i(x) := x^i/100$ for $i = 0, 1, 2, 3, 4$, where $x = [x^1, x^2, x^3, x^4]$ and $x^0 = 100 - \sum_{i=1}^{4} x^i$.

Once a biopsy is performed, the patient is only allowed to move to the posttreatment state, PT, or the perfect benign state, [0,0,0,0], depending on the outcome of the biopsy. Therefore, using the definition of $\rho^0(x_t)$, if the patient is in state x_t and has a biopsy at time t, we have $p_t([0, 0, 0, 0] \mid x_t, \text{Bx}) = \rho^0(x_t)$ and $p_t(PT|x_t, \text{Bx}) = 1 - \rho^0(x_t)$ for every $x_t \in \mathcal{X}$. If the outcome of a biopsy performed at time t is benign, then no further screening action is taken until the next decision epoch $t + 1$ (in 6 months) and the patient's state evolves through the transition probability $p_t(x'|\vec{0}, \text{Sf})$. If the actions is an annual mammogram, the transition probabilities can be computed using the one-step transition probability matrix of short-term follow-up action. That is, $p_t(x_{t+2}|x_t, \text{Am}) = \sum_{x_{t+1} \in \mathcal{X}} p_t(x_{t+1}|x_t, \text{Sf}) p_{t+1}(x_{t+2}|x_{t+1}, \text{Sf})$, where we define $p_t(x_{t+1}|x_t, \text{Am}) = 0$ if $x_{t+1} \neq x_t$ for all t.

We define death probabilities corresponding to different outcomes/diseases as follows.

Definition 2. $p_t^i(D)$ denotes the probability of death during the decision epoch t, when the patient is cancer-free, has low-grade DCIS, intermediate-grade DCIS, high-grade DCIS, and invasive cancer, for $i = 0, 1, 2, 3, 4$, respectively. Accordingly, if the patient is in state x_t and the action is Sf at time t, the probability of death is given by $p_t(D|x_t, \text{Sf}) =$

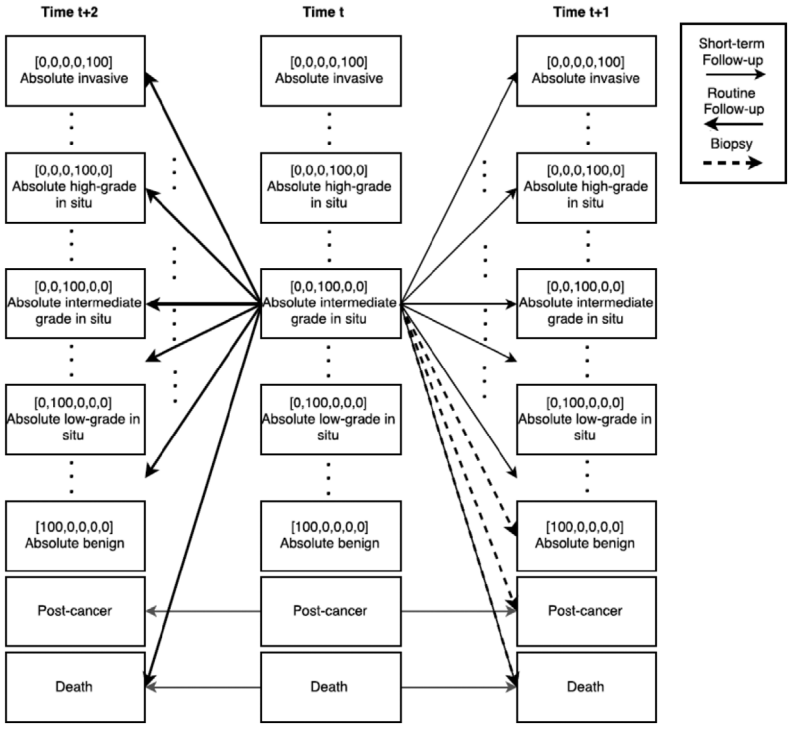

FIGURE 1 State transition diagram for the large-scale diagnostic decision model (LSM)

$\sum_{i=0}^{4} \rho^i(x_t) p_t^i(D)$. Similarly,

$$p_t(D|x_t, \text{Am}) = \sum_{x_{t+1} \in \mathcal{X} \cup \{D\}} p_t(x_{t+1}|x_t, \text{Sf}) p_{t+1}(D|x_{t+1}, \text{Sf}) = p_t(D|x_t, \text{Sf}) + \sum_{x_{t+1} \in \mathcal{X}} p_t(x_{t+1}|x_t, \text{Sf}) p_{t+1}(D|x_{t+1}, \text{Sf}). \tag{1}$$

We use QALYs to measure the benefit of postmammography actions capturing the patient survival and the associated quality of life (Drummond et al., 2015). QALYs associated with noninvasive imaging options, $r_t(x_t, \text{Sf})$ and $r_t(x_t, \text{Am})$, are calculated considering the possibility of death at any time during discrete time intervals to account for the half-cycle correction as follows:

$$r_t(x_t, \text{Sf}) = \frac{1}{2}(1 - p_t(D|x_t, \text{Sf})) + \frac{1}{4} p_t(D|x_t, \text{Sf}) - u_t(\text{Sf}) = \frac{1}{2} \sum_{i=0}^{4} \rho^i(x_t)(1 - p_t^i(D)) + \frac{1}{4} \sum_{i=0}^{4} \rho^i(x_t)(p_t^i(D)) - u_t(\text{Sf}), \tag{2}$$

where $u_t(\text{Sf})$ is the disutility associated with the short-term follow-up at decision epoch t. Similarly,

$$r_t(x_t, \text{Am}) = (1 - p_t(D|x_t, \text{Am})) + \frac{1}{2} p_t(D|x_t, \text{Am}) - u_t(\text{Am}), \tag{3}$$

where $u_t(\text{Am})$ is the disutility associated with annual mammogram at time t.

When a patient undergoes a biopsy, the QALYs accrued depend on the outcome of the biopsy. If the outcome is benign, then the patient moves to the $[0, 0, 0, 0]$ state and receives an intermediate reward, $r_t(x_t, \text{Bx}, B)$. If, on the other hand, the outcome is malignant, then the patient moves to state PT and receives a lump-sum reward, $r_t(x_t, \text{Bx}, C)$. We have $r_t(x_t, \text{Bx}, B) = \frac{1}{2}(1 - p_t^0(D)) + \frac{1}{4} p_t^0(D)$ and $r_t(x_t, \text{Bx}, C) = \sum_{i=1}^{4} \frac{\rho^i(x_t)}{1 - \rho^0(x_t)} r_t^i(\text{Bx})$, where $r_t^i(\text{Bx})$ is the expected postbiopsy reward when the patient is diagnosed with a cancer type i for $i = 1, 2, 3, 4$. Accordingly, the total QALYs associated with a biopsy at time t, $r_t(x_t, \text{Bx})$, is given by

$$r_t(x_t, \text{Bx}) = \rho^0(x_t) r_t(x_t, \text{Bx}, B) + (1 - \rho^0(x_t)) r_t(x_t, \text{Bx}, C) - u_t(\text{Bx}), \tag{4}$$

where $u_t(\text{Bx})$ is the disutility of biopsy. Although different preferences of older and younger patients toward mammography screening and biopsy may be modeled by defining time-dependent disutilities, we assume all disutilities are stationary in this study. Additionally, the effect of overtreatment can be introduced into the model by including an appropriate disutility associated with the estimated risk of overtreatment as a function of patient's age and type of cancer to the lump-sum reward received when the biopsy reveals a cancer with type i, that is, $r_t^i(\text{Bx})$. Finally, our model assumes that any diagnosed DCIS patient is treated with an appropriate

treatment and does not investigate the optimal treatment plan for these patients.

The optimal value function, $\mathcal{V}_t(x_t)$ can be calculated by solving the standard form of Bellman's equation (Puterman, 1994):

$$\mathcal{V}_t(x_t) = \max \Bigg\{ r_t(x_t, \text{Bx}) + \gamma \rho^0(x_t) \sum_{x' \in \mathcal{X}} p_t\big(x' | \vec{0}, \text{Sf}\big) \mathcal{V}_{t+1}(x'),$$
$$r_t(x_t, \text{Sf}) + \gamma \sum_{x' \in \mathcal{X}} p_t\left(x' | x_t, \text{Sf}\right) \mathcal{V}_{t+1}(x'),$$
$$r_t(x_t, \text{Am}) + \gamma^2 \sum_{x' \in \mathcal{X}} p_t\left(x' | x_t, \text{Am}\right) \mathcal{V}_{t+2}(x') \Bigg\}, \quad (5)$$

where $\gamma \in [0, 1]$ is the 6-month discount factor capturing the effect of timely decisions, $\vec{0} := [0, 0, 0, 0]$, $x_t \in \mathcal{X}$, and $t = 0, \ldots, T-2$. For $t = T-1$, the optimality equation becomes

$$\mathcal{V}_t(x_t) = \max \Bigg\{ r_t(x_t, \text{Bx}) + \gamma \rho^0(x_t) \sum_{x' \in \mathcal{X}} p_t\Big(x' | \vec{0}, \text{Sf}\Big)$$
$$\mathcal{V}_{t+1}(x'), \quad r_t(x_t, \text{Sf}) + \gamma \sum_{x' \in \mathcal{X}} p_t\big(x' | x_t, \text{Sf}\big) \mathcal{V}_{t+1}(x') \Bigg\}, \quad (6)$$

where $x_t \in \mathcal{X}$. Finally, for $t = T$, we introduce a boundary condition given by

$$\mathcal{V}_T(x_T) = r_T(x_T), \quad (7)$$

where $x_T \in \mathcal{X}$ and $r_T(x_T)$ denotes the extrapolated QALYs at the end of the decision horizon when the patient is in x_T. We define $a^*(x_t)$ as the optimal action corresponding to $x_t \in \mathcal{X}$ at time t.

4 | ALGORITHM DEVELOPMENT AND STRUCTURAL RESULTS

In this section, we present the details of the algorithm development and structural results related to the LSM as well as the solution algorithms. In its current form, the cardinality of the state space, which is approximately 4.6 million, makes the LSM computationally intractable. Therefore, we conduct a structural analysis of the LSM to develop computationally efficient algorithms.

In this context, we first introduce a DS algorithm in Section 4.1 to find an exact solution to the LSM by diving the large state space into smaller hyperplanes and evaluating only a small subset of the state space. Theorem 1 and Proposition 2 prove the optimality of the solution obtained by this algorithm. The complexity and performance of the DS algorithm highly depend on the upper bounds for the optimal biopsy decision thresholds, and accordingly, we develop a novel dimension reduction method to find such upper bounds in Section 4.2. Theorem 2 proves that the value functions obtained by our dimension reduction method provide upper bounds for the optimal biopsy decision thresholds in the LSM. We then use the results of Section 4.2 to implement the DS algorithm using the dimension reduction method and solve the LSM optimally in polynomial time.

For our structural analysis, we need an ordering of patients with respect to their cancer risk, but no simple method exists to rank the multidimensional risk vectors. We start with the following partial order definition that will be used throughout this section.

Definition 3. We define the *risk-based* order $\leq$ as a componentwise order on $\mathcal{X}$, so that for any $x, y \in \mathcal{X}$, $x \leq y$ if and only if $x_i \leq y_i$ for $i = 1, \ldots, 4$. The risk-based order is a partial order on $\mathcal{X}$.

Although not every pair of risk vectors are comparable under the risk-based order, we show that those observing the order exhibit significant structural properties. We also introduce a total order over the state space in the following definition.

Definition 4. We define the *reward-based* order $\underset{r}{\leq}$ imitating the reverse of the order between the intermediate and boundary rewards, so that $x \underset{r}{\leq} y$ if and only if $r_t(x, a) \geq r_t(y, a)$ for $a \in \{\text{Bx}, \text{Sf}, \text{Am}\}$ and $t = 0, 1, \ldots, T$, without loss of generality. This reward-based order is a total order over $\mathcal{X}$.

The total order defined in Definition 4 imitates the radiologist's assessment of a patient's condition under different risk states. Using such an order, we derive structural results on the optimal value functions over the entire state space, which are later used to prove fundamental results on the optimal actions for state pairs that are comparable under the risk-based order. Lemma 1 establishes that the risk-based order implies the reward-based order. The proofs of the remark as well as all other results in this paper are included in Online Appendix E.

Lemma 1. *For any $x, y \in \mathcal{X}$ if $x \leq y$, then $x \underset{r}{\leq} y$.*

The following list enumerates the major assumptions that are used throughout this section.

(A-1) The reward function $r_t(x_t, a)$ is nonincreasing in x_t with respect to the total order, for all $a \in \{\text{Bx}, \text{Sf}, \text{Am}\}$ and $t = 0, 1, \ldots, T$.

(A-2) The expected postbiopsy reward when the patient is diagnosed with a disease with type i, $r_t^i(\text{Bx})$ is nonincreasing in i for all $t = 0, 1, \ldots, T$.

(A-3) The transition probability matrices, $\mathbb{P}_t^{\text{Am}}$ and $\mathbb{P}_t^{\text{Sf}}$, are with increasing failure rate (IFR) (Barlow & Proschan, 1965) with respect to the total order, that is, $\sum_{y \underset{r}{\geq} x'} p_t(y|x, a)$ is nondecreasing in x for any $x' \in \mathcal{X}$, $a \in \{\text{Sf}, \text{Am}\}$ and $t = 0, 1, \ldots, T$.

Assumption (A-3) is a widely used assumption on transition probability matrices to analyze the structure of the optimal policy in the optimization literature (Chhatwal et al., 2010; Puterman, 1994). The following proposition proves the monotonicity of the optimal value function, $\mathcal{V}_t(x)$, with respect to the reward-based order over the entire state space:

Proposition 1. *For any $x, y \in \mathcal{X}$ and $t = 0, 1, \ldots, T$, if $x \underset{r}{\leq} y$, then $\mathcal{V}_t(x) \geq \mathcal{V}_t(y)$.*

We next provide an upper bound, Z_t^{max}, and a lower bound, $r_t^A(\text{Bx})$, on $\mathcal{V}_t(x)$ for any $x \in \mathcal{X}$ in Lemma 2, and defer intuitive explanation of these bounds until after Theorem 1.

Lemma 2. *For any $x \in \mathcal{X}$ and $t = 0, 1, \ldots, T$, let Z_t^{max} be recursively defined as*

$$Z_t^{max} = \max\Big\{ r_t(\vec{0}, Sf) + \gamma(1 - p_t^0(D))Z_{t+1}^{max}, r_t(\vec{0}, Am) + \gamma^2(1 - p_t^0(D, Am))Z_{t+2}^{max} \Big\}, \tag{8a}$$

$$Z_{T-1}^{max} = r_{T-1}(\vec{0}, Sf) + \gamma(1 - p_{T-1}^0(D))Z_T^{max}, \tag{8b}$$

$$Z_T^{max} = r_T(\vec{0}), \tag{8c}$$

then the optimal value function $\mathcal{V}_t(x)$ satisfies

$$Z_t^{max} \geq \mathcal{V}_t(x) \geq r_t(x, Bx, C). \tag{9}$$

Our main result in this section is provided in Theorem 1, which exploits the risk-based order among different states to compare the optimal actions of a pair of states that are comparable under the risk-based order.

Theorem 1. *For any t and $i \in \{1, 2, 3, 4\}$, if Z_t^{max}, $r_t(x, Bx, C)$, and $r_t(x, Bx)$ satisfy the following condition:*

$$10^{-2} \cdot \Big[\big(1 - p_t^0(D)\big) \cdot Z_{t+1}^{max} - \big(p_t^i(D) - p_t^0(D)\big) \times r_{t+1}(x + e_i, Bx, C)\Big] \leq r_t(x + e_i, Bx) - r_t(x, Bx), \tag{10}$$

where e_i denotes the vector with a 1 in the ith coordinate and 0 elsewhere, then for any $x_t \leq y_t$, if $a^*(x_t) = Bx$, then $a^*(y_t) = Bx$.

For an intuitive interpretation of inequality (10), first observe that Z_t^{max} defined in Equation (8) represents the expected life of a patient with zero risk of cancer if she remains at zero risk and never has a biopsy starting from time t, and $r_t(x_t, \text{Bx}, C)$ represents the expected postbiopsy reward when the patient receives a biopsy with a malignant outcome. Recall from the optimality equations in (5) that the reward of the biopsy action includes the immediate and lump-sump rewards associated with the biopsy as well as the expected benefit from continuing the decision process after a benign outcome. Inequality (10) implies that when the risk of malignancy slightly increases by 1%, with a probability of 1%, the marginal benefit of biopsy should be higher than the difference between the expected additional benefits of receiving a benign biopsy outcome, surviving the next decision epoch, and spending the rest of life with no risk of cancer (as represented by $(1 - p_t^0(D)) \cdot Z_{t+1}^{max}$) and the expected reduced benefits of surviving the next decision epoch and receiving a malignant biopsy outcome (as represented by $(p_t^i(D) - p_t^0(D)) \cdot r_{t+1}(x + e_i, \text{Bx}, C)$.

Theorem 1 significantly reduces the complexity of solving the LSM by reducing the search space for the optimal action iteratively. While there exists no obvious method to create a single scalar threshold for the optimal actions in the LSM due to its multidimensional state space, Theorem 1 provides multiple biopsy thresholds that can be used to develop a computationally tractable algorithm to find an exact optimal solution to the LSM.

We next develop and prove the optimality of an algorithm that relies on Theorem 1 to find an exact optimal solution to the LSM in Section 4.1.

4.1 | DS Algorithm

We next develop an algorithm to solve the LSM optimally in polynomial time. Section 4 established a method to correlate the optimal actions of states that are comparable under the risk-based order, however, not all states in the multidimensional state space of LSM are comparable under the given risk-based order. Our approach in developing a polynomial-time solution algorithm involves finding an appropriate partition of the state space into smaller sets, which are comparable with each other at least over some of their elements, in such a way that determining the optimal action for a manageable number of these sets would suffice to deduce the optimal action for the entire state space. In that respect, we begin with separating the large state space into smaller segments by creating sets of states according to their nonbenign (i.e., malignancy) probabilities in Definition 5.

Definition 5. Let Σ_k be defined as the set of state vectors with total nonbenign probability of $k/100$, where $k \in \{0, \ldots, 100\}$, that is, $\Sigma_k := \{x \in \mathcal{X} | x^1 + x^2 + x^3 + x^4 = k\}$.

The choice of hyperplanes in Definition 5 is of particular interest to our model because for any state vector $y \in \Sigma_\ell$ with $\ell > k$, there exists at least one vector $x \in \Sigma_k$ that is comparable to y under the risk-based order. In other words, for any $\ell > k$, the hyperplane Σ_ℓ contains states that have a higher risk of malignancy compared to at least some in Σ_k. Therefore, if one can identify a hyperplane that consists of states for which the optimal action is a biopsy, which we refer as a *full-biopsy hyperplane*, then the results of Theorem 1 can be used to conclude that any hyperplane with a greater index

ALGORITHM 1 Divide-and-Search (DS) Algorithm

Step 0: Initialize

The terminal rewards $v_T(x_T)$.

Set $t = T - 1$ and $k = 1$

Step 1: Calculate for $x_t \in \Sigma_i$

(i): $r_t(x_t, Am) + \gamma^2 \sum_{x' \in \mathcal{X}} p_t(x'|x_t, Am)\mathcal{V}_{t+2}(x')$

(ii): $r_t(x_t, Sf) + \gamma \sum_{x' \in \mathcal{X}} p_t(x'|x_t, Sf)\mathcal{V}_{t+1}(x')$

(iii): $r_t(x_t, Bx) + \gamma\rho^0(x_t) \sum_{x' \in \mathcal{X}} p_t(x'|\vec{0}, Sf)\mathcal{V}_{t+1}(x')$

Step 2: Determine

the maximum of (i)–(iii) in Step 1 to set $a_t^*(x_t)$ and $\mathcal{V}_t(x_t)$ for $x_t \in \Sigma_k$

Step 3: Analyze

if $a_t^*(x_t) = Bx$ for all $x_t \in \Sigma_i$ **then**

Set $a_t^*(x_t) = Bx$ and $\mathcal{V}_t(x_t) = r_t(x_t, Bx) + \gamma\rho^0(x_t) \sum_{x' \in \mathcal{X}} p_t(x'|\vec{0}, Sf)$ $\mathcal{V}_{t+1}(x')$ for all $x_t \in \Sigma_\ell$, $\ell > k$. And set biopsy cut-off $k_t = k$

else

Increment k and return to step 1

end if

Step 4: Observe

if $t > 0$ **then**

Decrement t.

If there exists an upper bound K_t on the biopsy cut-off k_t, skip the calculation of $p_t(x'|x_t, a)$ for all $a \in \{Sf, Am\}$, $x_t \in \Sigma_k$, $k \geq K_t$, return to step 1

else

Stop.

end if

should also be a full-biopsy hyperplane. Proposition 2 formally proves this observation, which plays a key role to solve the LSM optimally in polynomial time.

Proposition 2. *For any $t \in [0, T]$ and $k \in \{0, \ldots, 100\}$, if $a_t^*(x_t) = Bx$ for all $x_t \in \Sigma_k$, then $a_t^*(y_t) = Bx$ for all $y_t \in \Sigma_\ell$ with $\ell \geq k$, given that inequality (10) holds.*

Among full-biopsy hyperplanes, identifying the one with the smallest index is important to establish the minimum number of states that need to be evaluated to determine the optimal actions for the entire state space. Let k_t denote this smallest index at time t, which we refer to as the biopsy cut-off at time t. The result provided in Proposition 2 implies that for any $\ell \geq k_t$, Σ_ℓ should be a full-biopsy hyperplane.

We are now ready to formally present the solution algorithm in Algorithm 1. At each decision epoch, the algorithm first divides the state space into hyperplanes, and then, starting with the ones that consist of states with a high probability of being cancer-free, it determines the optimal actions and value functions for each state in a hyperplane. By targeting the hyperplanes with a lower probability of malignancy, the algorithm aims to enclose the set of states for which a biopsy is optimal. DS algorithm provides a variant of the divide-and-conquer approach and integrates a selective nature to the conventional backward induction method, which would exhaustively search the optimal actions of all 4.6 million states. The algorithm iteratively divides the large state space into smaller comparable sets and performs a selective search through only a few of these sets. The selective search strategy significantly reduces the computational complexity as the calculation of a limited number of optimal value functions suffices to provide the optimal actions for all states.

At each decision epoch, Algorithm 1 starts with the set of states Σ_0, which consists of only the [0,0,0,0] state, and continues to search for the optimal actions corresponding to the states that belong to Σ_i for $i = 1, 2, \ldots$ until it stops at the first full-biopsy hyperplane Σ_{k_t}. As a trivial example, when $k_t = 2$, Algorithm 1 starts with the [0,0,0,0] state to observe that the corresponding optimal action is not biopsy. Then it continues with Σ_1, which consists of the [1,0,0,0], [0,1,0,0], [0, 0, 1, 0], and [0,0,0,1] states, to observe that the optimal action for at least one of the states is again not biopsy. Finally, the algorithm continues with Σ_2 only to identify that the optimal action for all of the states in the set is biopsy, then the algorithm stops and directly assigns the optimal actions for the rest of the states in Σ_k for $k > 2$. Here, identifying the biopsy cutoff k_t is the first step on reducing the computational complexity. Once k_t is identified, we can calculate the optimal actions and value functions of the states that belong to Σ_j with $j \geq k_t$ in $\mathcal{O}(|\mathcal{X}|)$.

When Algorithm 1 stops at a biopsy cutoff k_t, it assigns the optimal action for any state belonging to Σ_i with $i > k_t$ as biopsy without further evaluation. For any given k_t, Algorithm 1 sets $\mathcal{V}_t(x_t) = r_t(x_t, \mathrm{Bx}) + \gamma\rho^0(x_t) \sum_{x' \in \mathcal{X}} p_t(x'|\vec{0}, \mathrm{Sf})\mathcal{V}_{t+1}(x')$ for any $x_t \in \Sigma_i$ with $i > k_t$. Since the inner product $\sum_{x' \in \mathcal{X}} p_t(x'|\vec{0}, \mathrm{Sf})\mathcal{V}_{t+1}(x')$ does not depend on x_t, the calculation of $\mathcal{V}_t(x_t)$s for all $x_t \in \Sigma_i$ with $i > k_t$ only requires a scalar multiplication and a summation for any $x_t \in \Sigma_i$ with $i > k$, and therefore, it can be done in linear time. Considering that the number of elements of the set Σ_i is $\binom{i+3}{3}$, at each decision epoch t, Algorithm 1 explicitly calculates the optimal actions and the value functions of only $\binom{k_t+4}{4}$ states in total. For the remaining $\binom{104}{4} - \binom{k_t+4}{4}$ states, the optimal actions and value functions are set in linear time.

Step 4 of Algorithm 1 checks if there exists any upper bound on the biopsy cutoff k_t exogenously fed to the algorithm, and if so, it skips the calculation of the transition probabilities $p_t(x'|x_t, a)$ for all $a \in \{\mathrm{Sf}, \mathrm{Am}\}$, $x_t \in \Sigma_i$, $i > k_t$. As a result, Step 4 can provide a further reduction in the time and memory complexity of the algorithm if we are able to identify tight upper bounds on k_t at time t. We provide such upper bounds in Section 4.2 by implementing alternative MDP models using dimension reduction on the original state space.

4.2 | Dimension reduction method

To provide upper bounds on the biopsy cutoff k_t in Algorithm 1, we introduce alternative MDP models with a smaller

state space by projecting the state space of the LSM onto a lower dimension. We refer to these alternative MDPs as reduced dimension diagnostic decision models (RDMs), namely, the RDM-upper and the RDM-lower, and use them to obtain feasible bounds on the optimal value functions and biopsy cutoff, k_t, of the DS algorithm given in Section 4.1. Accordingly, the RDM-upper and RDM-lower supplement the LSM by significantly improving the complexity of its optimal solution algorithm.

The dimension reduction is accomplished by merging different DCIS grades into a single DCIS category, and therefore, projecting five-dimensional state space onto three-dimensional space.[3] The (reduced-dimension) state space of the RDM-upper and RDM-lower is defined as follows:

$$\mathcal{P}\bar{\mathcal{X}} := \left\{ [y^0, y^1, y^2] \;\middle|\; y^0 = x^0, y^2 = x^4, y^1 = \sum_{i=1}^{3} x^i,\ [x^0 x^1 x^2 x^3 x^4] \in \bar{\mathcal{X}} \right\}, \tag{11}$$

where the posttreatment state and the death states are preserved through the projection $\mathcal{P}$. The number of states in the reduced-dimension problems, which equals $\binom{102}{2} + 2 = 5153$, is significantly lower than the number of states in the LSM, which is around 4.6 million, and this allows the exact calculation of the optimal value functions of the RDM-upper and RDM-lower.

At each decision epoch $t = 0, 1, \ldots, T$, $Q_t = [q_t(.|.)]$ and $\widetilde{Q}_t = [\widetilde{q}_t(.|.)]$ represent the transition probability matrices, $\tau_t(y_t, a)$ and $\widetilde{\tau}_t(y_t, a)$ represent the intermediate expected rewards accrued when the patient is in state $y_t \in \mathcal{P}\bar{\mathcal{X}}$ and action $a \in \{\text{Bx}, \text{Sf}, \text{Am}\}$ is recommended, and finally $\mathfrak{v}_t(y_t)$ and $\widetilde{\mathfrak{v}}_t(y_t)$ represent the optimal value functions of state $y_t \in \mathcal{P}\bar{\mathcal{X}}$ in the RDM-upper and the RDM-lower, respectively. The details of the selection and estimation of the parameters for the reduced dimension problems are given in Section 5. The optimality equations for the RDM-upper and the RDM-lower are similar to those of the LSM given in Section 3 and are omitted for the brevity of presentation.

Definition 6 introduces a concept similar to stochastic dominance to compare the transition probability matrix of the LSM with those of the RDM-upper and the RDM-lower. It compares the transition probabilities from y_t in the reduced dimension space $\mathcal{P}\bar{\mathcal{X}}$ with the probabilities from the set of states in the original space $\bar{\mathcal{X}}$, which are projected to y_t under the projection $\mathcal{P}$.

Definition 6. A transition probability matrix $Q = [q(.|.)]$ of the RDM-lower *dominates* the transition probability matrix $P = [p(.|.)]$ of the LSM if $q(y'|y, a) \geq \max_{x \in \mathcal{P}^{-1}y} \sum_{x' \in \mathcal{P}^{-1}y'} p(x'|x, a)$ for all y', $y \in \mathcal{P}\bar{\mathcal{X}}$, and $a \in \{\text{Sf}, \text{Am}\}$, where $\mathcal{P}^{-1}$ is defined as the inverse projection given by

$$\mathcal{P}^{-1}[y^0, y^1, y^2] := \left\{ x \in \bar{\mathcal{X}} | x^0 = y^0, x^4 = y^2, \sum_{i=1}^{3} x^i = y^1 \right\}. \tag{12}$$

Similarly, $\widetilde{Q}$ is *dominated by* P if $\widetilde{q}(y'|y, a) \leq \min_{x \in \mathcal{P}^{-1}y} \sum_{x' \in \mathcal{P}^{-1}y'} p_t(x'|x, a)$ for all y', $y \in \mathcal{P}\bar{\mathcal{X}}$, and $a \in \{\text{Sf}, \text{Am}\}$.

In Section 5, we present the details of the estimation of the transition probability matrices P_t, Q_t, and $\widetilde{Q}_t$ for any t. We further prove in Section 5 that the given estimations of P_t, Q_t, and $\widetilde{Q}_t$ provide an example of a Q_t that dominates P_t, and a $\widetilde{Q}_t$ that is dominated by P_t at any time t. Since the definitions of Q_t and $\widetilde{Q}_t$ given in Section 5 do not require the calculation of P_t, Algorithm 1 can use the bounds provided by the RDM-upper and RDM-lower on the biopsy cutoff defined in Section 4.1, and skip the calculation and storage of a substantial portion of 4.6 million rows of P_t, significantly reducing the time and memory complexity.

Proposition 3 presents upper and lower bounds on the optimal value functions of the LSM using those of the RDM-upper and RDM-lower.

Proposition 3. *For any $t = 0, 1, \ldots, T$, if Q_t dominates P_t, $\widetilde{Q}_t$ is dominated by P_t, and $\tau_t(y_t, a)$, $r_t(x_t, a)$, and $\widetilde{\tau}_t(y_t, a)$ satisfy the following assumption:*

$$\tau_t(y_t, a) \geq r_t(x_t, a) \geq \widetilde{\tau}_t(y_t, a) \tag{13}$$

for all $y_t \in \mathcal{P}\bar{\mathcal{X}}$, $x_t \in \mathcal{P}^{-1}y_t$, and $a \in \{Bx, Sf, Am\}$, then the following inequalities hold,

$$\begin{aligned} \mathfrak{v}_t(y_t) &\geq \mathcal{V}_t(x_t), \\ \widetilde{\mathfrak{v}}_t(y_t) &\leq \mathcal{V}_t(x_t), \end{aligned} \tag{14}$$

for all $y_t \in \mathcal{P}\bar{\mathcal{X}}$, $x_t \in \mathcal{P}^{-1}y_t$.

The bounds provided in Proposition 3 will be next used in Theorem 2 to find an upper bound on the biopsy cutoff of the DS algorithm. Proposition 3 can further be used to approximate the optimal value functions for other large-scale problems for which the application of the DS algorithm is not feasible. Such an approximation would be particularly useful in problems, where, for example, the decision maker is interested in assessing the efficiency of a policy by estimating its expected QALY gains. Additionally, if the biopsy cutoff k_t given in Algorithm 1 were found to be too high that no efficient method to calculate the exact optimal solution exists, then Proposition 3 could be used to provide an approximate optimal solution to the LSM.

Theorem 2 presents the sufficient conditions for the optimal solutions of the RDM-upper and RDM-lower to provide an upper bound on the biopsy cutoff of the DS algorithm.

Theorem 2. *For any t, if Q_t dominates P_t, $\widetilde{Q}_t$ is dominated by P_t, and (13) holds for all $y_t \in \mathcal{P}\bar{\mathcal{X}}$, $x_t \in \mathcal{P}^{-1}y_t$, $a \in \{Bx, Sf, Am\}$, then for any $y_t \in \mathcal{P}\bar{\mathcal{X}}$ satisfying the following inequality:*

$$\widetilde{\tau}_t(y_t, Bx) + \gamma\rho^0(y_t) \sum_{y' \in \mathcal{P}\bar{\mathcal{X}}} \widetilde{q}_t(y'|\vec{0}, Sf)\widetilde{\mathfrak{v}}_{t+1}(y')$$

$$\geq \max\left\{ \tau_t(y_t, Sf) + \gamma \sum_{y' \in \mathcal{P}\bar{\mathcal{X}}} q_t(y'|y_t, Sf)\mathfrak{v}_{t+1}(y'), \right.$$

$$\left. \tau_t(y_t, Am) + \gamma^2 \sum_{y' \in \mathcal{P}\bar{\mathcal{X}}} q_t(y'|y_t, Am)\mathfrak{v}_{t+2}(y') \right\}, \quad (15)$$

$a^*(x_t) = Bx$ for all $x_t \in \mathcal{P}^{-1}y_t$ in the LSM. Therefore, for any K, if (15) is satisfied by $\forall\, y_t \in \mathcal{P}\Sigma_K$, then $\boldsymbol{k_t \leq K}$ holds, where k_t is the biopsy cutoff defined in Section 4.1.

Theorem 2 utilizes the bounds on the optimal value functions of the LSM given by Proposition 3 to derive the desired upper bounds. As a direct consequence of Theorem 2, the optimal solutions of the RDM-upper and RDM-lower can be used to reveal any $y_t \in \mathcal{P}\bar{\mathcal{X}}$ satisfying (15) and, therefore, to produce an upper bound on k_t, which can be augmented in Algorithm 1 to achieve a significant complexity reduction. In addition to the time complexity of the DS algorithm introduced in Section 4.1, the calculation and the storage of the large-scale transition matrix of the LSM also require intensive computational effort. The upper bound provided by Theorem 2 on k_t, further allows skipping the calculation and storage of a significant fraction of these transition probabilities at every decision epoch t, and substantially reduces both the time and memory complexity of the DS algorithm. For an upper bound of K on k_t, we skip the calculation and storage of $\binom{104}{4} - \binom{K+4}{4}$ transition probability vectors of size $\binom{104}{4}$ at decision epoch t. The largest upper bound we obtained on the biopsy cutoff for all ages is 16, which is consistent with the practical observations. Comparing the number of states sufficient to find the optimal policy at the worst case, which is $\binom{20}{4} = 4845$, to the total number of states, which is $\binom{104}{4} \approx 4.6$ million, demonstrates the magnitude of the reduction in the complexity gained by taking advantage of the upper bounds obtained by the dimension reduction method in optimally solving the LSM.

In Section 5, we provide the details of our parameter selection for the LSM, RDM-upper, and RDM-lower, and prove in Lemma 3 that P_t, Q_t, and $\widetilde{Q}_t$ defined in Section 5 satisfy the necessary conditions given in Theorem 2. Therefore, Section 5 concludes the dimension reduction algorithm by providing sufficient parameters to obtain an upper bound on the biopsy cutoff of the DS algorithm. Note that, since the results of Proposition 3 and Theorem 2 hold for any RDM-upper and RDM-lower satisfying the assumptions on the transition matrices, they have a broader range of applications rather than being limited to our setup.

5 | PARAMETER ESTIMATION

In this section, we present the data sources and the estimation of the parameters. Section 5.1 describes the sources of the clinical data that are used in our numerical study, and Section 5.2 presents the details of the estimation of transition probabilities and rewards for the LSM, the RDM-upper, and the RDM-lower, respectively. Further details of parameter estimation are presented in Online Appendix A.

5.1 | Data sources

There are five sources for our model parameters:

- *University of Wisconsin-Madison* (*UW*) *and University of California, San Francisco* (*UCSF*) *Data*: These private data sets include consecutive mammograms collected at the University of Wisconsin-Madison and University of California, San Francisco, which we utilize for our numerical results. Initially, we obtained two large data sets of consecutively collected mammography practices; 41,682 mammograms collected between January 1, 2006, and December 31, 2012, at UW and 146,996 mammograms collected between January 7, 1997, and December 18 2007, at UCSF. From these large data sets, we extracted 5607 biopsies based on the descriptors and final assessment categories that specify the cancer type. We also verified the outcomes through state cancer registries that systematically record cancer cases and incorporate false negatives, that is, malignant cases that are missed during the lecture of mammograms. Combining these two data sets from UW and UCSF allows us to demonstrate the generalizability of our computational results among different practices and provides us a unique breast cancer data set that has several novel components including breast cancer types. To the best of our knowledge, our database is the largest in the United States with information regarding breast cancer types and registry matching.
- *U.S. Life Tables*: 2011 United States life tables reported by the Centers for Disease Control and Prevention (CDC) (Arias, 2015). These tables are used to estimate age-specific mortality for patients with no breast cancer.
- *SEER Data*: This data set includes breast cancer survival statistics from the Surveillance, Epidemiology, and End Results (SEER) program of the NCI, (Siegel et al., 2015). We used this data set to estimate the age-specific probabilities of death from breast cancer as well as the age-dependent lump-sum postbiopsy rewards.
- *University of Wisconsin Breast Cancer Simulation* (*UWBCS*) *Model*: The UWBCS is a member of the

Cancer Intervention and Surveillance Modeling Network (CISNET), a consortium of NCI-sponsored groups using statistical modeling to evaluate the impact of cancer control interventions on population trends, and to help establish the optimal cancer control policies (Alagoz et al., 2018b). The UWBCS is a discrete-event, stochastic simulation model that analyzes breast cancer incidence and mortality in the United States and can address significant policy questions regarding breast cancer screening, diagnosis, and treatment. The UWBCS model has been calibrated to the breast cancer incidence and survival data reported by the SEER program and cross-validated against data from a state's Cancer Reporting System. The U.S. Preventive Services Task Force (USPSTF) used CISNET models, including UWBCS, to set the breast cancer screening policy in the United States both in 2009 and in 2016 (Alagoz et al, 2018a). We used the UWBCS simulation model to examine the comparative effectiveness of the optimal breast cancer diagnostic policies on a population level.

- *Risk Prediction Models*: These models predict the risk of cancer as a multidimensional risk vector, which includes the risk of aggressive and indolent types of cancers. The risk predictions are based on mammographic features and demographic risk factors using a multivariate logistic regression model (details are provided in Online Appendix C) and a tree augmented naive Bayes network (Kuusisto, 2015). These models are used alongside with the UW and UCSF data in estimating the transition probabilities as well as in the numerical illustration of our findings.

5.2 | Parameter estimation

We use the rates of progression between different breast cancer types to calculate the one-step transition probability matrix. Let δ_{ij} represent the 6-month probability of progression from i to j for $0 \le i < j \le 4$, where 0 represents being cancer-free, 1 represents the occurrence of low-grade DCIS, 2 represents the occurrence of intermediate-grade DCIS, 3 represents the occurrence of high-grade DCIS, and 4 represents the occurrence of invasive cancer.

Then, we define the one-step transition probability from state $x = [x^0, x^1, x^2, x^3, x^4]$ to $y = [y^0, y^1, y^2, y^3, y^4]$ given that the action is Sf at time t using multinomial distribution as

$$p_t(y|x, \text{Sf}) = \sum_{i=(y^1-x^1)^+}^{\zeta_1} \sum_{j=(y^2-x^2)^+}^{\zeta_2} \sum_{k=(y^3-x^3)^+}^{\zeta_3} \binom{x^0}{i} \binom{x^0-i}{j} \binom{x^0-i-j}{k} \binom{x^0-i-j-k}{x^0-y^0-i-j-k} \delta_{01}^{i}\, \delta_{02}^{j}\, \delta_{03}^{k}\, \delta_{04}^{x^0-y^0-i-j-k}\, \delta_{00}^{y^0} \binom{x^1}{x^1-y^1-i} \delta_{11}^{y^1-i}$$

$$\delta_{14}^{x^1-y^1+i} \binom{x^2}{x^2-y^2-j} \delta_{22}^{y^2-j}\, \delta_{24}^{x^2-y^2+j} \binom{x^3}{x^3-y^3-k} \delta_{33}^{y^3-k}\, \delta_{34}^{x^3-y^3+k}, \quad (16)$$

where $\zeta_1 := \min\{y^1, y^1 + y^4 - x^1 - x^4, x^0 - (y^2 - x^2)^+ - (y^3 - x^3)^+\}$, $\zeta_2 := \min\{y^2, y^1 + y^2 + y^4 - x^1 - x^2 - x^4 - i, x^0 - i - (y^3 - x^3)^+\}$, $\zeta_3 := \min\{y^3, y^1 + y^2 + y^3 + y^4 - x^1 - x^2 - x^3 - x^4 - i - j, x^0 - i - j\}$, and, f^+ and f^- are positive and negative parts of a function f, respectively. The transition probability given in (16) is estimated using the probability of having y^0 benign, y^1 low-grade DCIS, y^2 intermediate-grade DCIS, y^3 high-grade DCIS, and y^4 invasive findings at time $t+1$, when we have x^0 benign, x^1 low-grade DCIS, x^2 intermediate-grade DCIS, x^3 high-grade DCIS, and x^4 invasive findings at time t.

For the RDM-lower defined in Section 4.2, the one-step transition probability from state $x = [x^0, x^1, x^2]$ to $y = [y^0, y^1, y^2]$ given that the Sf action is chosen at time t is similarly defined using multinomial distribution as

$$q_t(y|x, \text{Sf}) = \sum_{i=(x^0+x^2-(y^0+y^2))^+}^{x^0-y^0-(-x^1-x^2+y^2)^+} \binom{x^0}{i} \binom{x^0-i}{x^0-y^0 i} \delta_{0D}^{i}\, \delta_{04}^{x^0-y^0-i} \delta_{00}^{y^0} \binom{x^1}{x^1-y^1+i} \delta_{D4}^{i+x^1-y^1}\, \delta_{DD}^{y^2-i}, \quad (17)$$

where δ_{0D} represents the 6-month probability of progression from benign to DCIS, δ_{D4} represents the 6-month probability of progression from DCIS to invasive, and δ_{DD} represents the probability of not progressing from DCIS to invasive in 6 months. The definition of one-step transition probability of the RDM-upper, $\widetilde{q}_t(y|x, \text{Sf})$, is similar to (17), with a small adjustment that $\widetilde{\delta}_{0D}$, $\widetilde{\delta}_{DD}$, and $\widetilde{\delta}_{D4}$ replace δ_{0D}, δ_{DD}, and δ_{D4} in (17), respectively. We define $\delta_{0D} = \widetilde{\delta}_{0D} = \sum_{i=1}^{3} \delta_{0i}$, $\delta_{D4} = \max_{i\in\{1,2,3\}} \delta_{i4}$, and $\widetilde{\delta}_{D4} = \min_{i\in\{1,2,3\}} \delta_{i4}$.

To validate our approximation of the one-step transition probability matrix, we calculated the lifetime risk of being diagnosed with breast cancer for a 40-year-old woman given that she is cancer-free at her current age. We found that the lifetime risk of invasive cancer approximated by our one-step transition probability matrix, 12.46%, is comparable to one reported by the NCI, 12.17% (Howlader et al., 2016). We also calculated the risk of being diagnosed with breast cancer in 10 years for a 60-year-old woman using our transition probability matrix, and again observed that the 10-year risk of invasive cancer approximated by our transition probability matrix, 3.35%, is comparable to the one reported by the NCI, 3.46%.

In Lemma 3, we prove that $P_t = [p_t(.|.)]$, as defined in (16), and $Q_t = [q_t(.|.)]$ and $\widetilde{Q}_t = [\widetilde{q}_t(.|.)]$, as defined in (17), satisfy the necessary conditions of Theorem 2 for any t. Lemma 3 allows the use of the RDM-upper and RDM-lower in obtaining feasible upper bounds for the LSM.

Lemma 3. *Let* $P_t = [p_t(.|.)]$, $Q_t = [q_t(.|.)]$, *and* $\widetilde{Q}_t = [\widetilde{q}_t(.|.)]$ *be defined by* (16), (17), *and the modified version of* (17), *respectively. Then, for any* y', $y_t \in \mathcal{P}\tilde{\mathcal{X}}$, *the following inequalities hold:*

$$q_t(y'|y_t, a) \geq \max_{x_t \in \mathcal{P}^{-1} y_t} \sum_{x' \in \mathcal{P}^{-1} y'} p_t(x'|x_t, a), \tag{18}$$

$$\widetilde{q}_t(y'|y_t, a) \leq \min_{x_t \in \mathcal{P}^{-1} y_t} \sum_{x' \in \mathcal{P}^{-1} y'} p_t(x'|x_t, a), \tag{19}$$

where $a \in \{Sf, Am\}$.

Finally, the rewards of the RDM-lower, $\tau_t(y_t, a)$, and RDM-upper, $\widetilde{\tau}_t(y_t, a)$, for $a \in \{\text{Bx}, \text{Sf}, \text{Am}\}$, are set as follows:

$$\tau_t(y_t, a) = \max_{x_t \in \mathcal{P}^{-1} y_t} r_t(x_t, a) \quad \text{and}$$

$$\widetilde{\tau}_t(y_t, a) = \min_{x_t \in \mathcal{P}^{-1} y_t} r_t(x_t, a). \tag{20}$$

6 | NUMERICAL RESULTS

In this section, we provide our numerical results using the clinical data. First, we provide the optimal age-specific diagnostic policies based on a patient's risk of low-, intermediate-, high-grade DCIS, and invasive cancer using the LSM. Then, we incorporate the optimal policies of the LSM into the UWBCS simulation model to examine the comparative effectiveness of the optimal breast cancer diagnostic policies on a population level. Thus, we estimate the potential rate of reduction in overdiagnosis obtained by following the optimal multidimensional diagnostic guidelines over the current clinical practice. Finally, we evaluate the value of our modeling and solution approach by comparing the performance of the LSM to that of a conventional optimization model, which ignores breast cancer types and only includes a scalar state to represent breast cancer.

6.1 | Optimal diagnostic policies

The high dimensionality of the state space limits the presentation of the optimal diagnostic policies as a function of DCIS risks only to several risk levels of invasive cancer for certain ages. Figure 23 provide the optimal diagnostic strategies as a function of low-, intermediate-, and high-grade DCIS risks for various ages when the risk of invasive cancer is 0% and 1%, respectively. To demonstrate the patterns observed in the optimal strategies, the optimal diagnostic policies are only provided for selected ages. The optimal diagnostic policies corresponding to the cases where the risk of invasive cancer is higher than 1% are omitted here and summarized in a compact form later in this section.

In Figure 23, the X, Y, and Z axes represent the percentage risk of high-, intermediate-, and low-grade DCIS, respectively. Since the risk of invasive cancer is fixed in these figures, the probability of being cancer-free can be calculated by subtracting the sum of these probabilities from 1. The surfaces in Figure 2 and Figure 3 represent the biopsy and short-term follow-up thresholds such that for any state below the short-term follow-up threshold surface, the optimal action is annual mammography; for any state between the two threshold surfaces, the optimal action is the short-term follow-up; and, for any state above the biopsy threshold surface, the optimal action is a biopsy. Figure 2 and Figure 3 illustrate a significant discrepancy between the biopsy thresholds of low-, intermediate-, and high-grade DCIS with an increasing trend as the patients get older.

Figure 4 presents the age-specific optimal diagnostic policies as a function of aggregate DCIS risks for various risk levels of invasive cancer to better illustrate the effect of age on the optimal diagnostic thresholds. This compact presentation further allows demonstrating the optimal thresholds when the risk of invasive cancer is higher than 1%. In Figure 4, the horizontal axis represents the age and the vertical axis represents the aggregate probability of DCIS. Figure 4 shows that the optimal diagnostic thresholds in terms of aggregate DCIS

(i) increase with increasing age at any level of invasive cancer risk and
(ii) decline with increasing risk of invasive cancer, so that at 3% risk of invasive cancer the optimal action is biopsy for all patients younger than 75 regardless of their risk of DCIS.

Therefore, Figure 4 implies that the current diagnostic guidelines of biopsying any findings with more than 2% probability of cancer would be optimal *only if* the findings clearly indicate aggressive cancer. These findings highlight that neglecting the age-specific differences between indolent and invasive types of breast cancer in making diagnostic decisions results in aggressive biopsy decisions, and we next show in Section 6.2 that these aggressive biopsy decisions not only reduce the quality of life in patients who would be better off with noninvasive imaging but also lead to significant rates of overdiagnosis.

6.2 | The population impact of the optimal diagnostic policies from the LSM

In the current clinical practice, diagnostic decisions are made through a scalar risk of cancer, which corresponds to the cumulative sum of the risks of low-, intermediate-, high-grade DCIS, and, invasive cancer, where a decision threshold of 2% is used for biopsy recommendations regardless of patient's age or breast cancer type (BI-RADS, 2003). Our numerical findings confirm our initial hypothesis that ignoring age-specific differences between indolent and aggressive cancers in setting a biopsy threshold may significantly

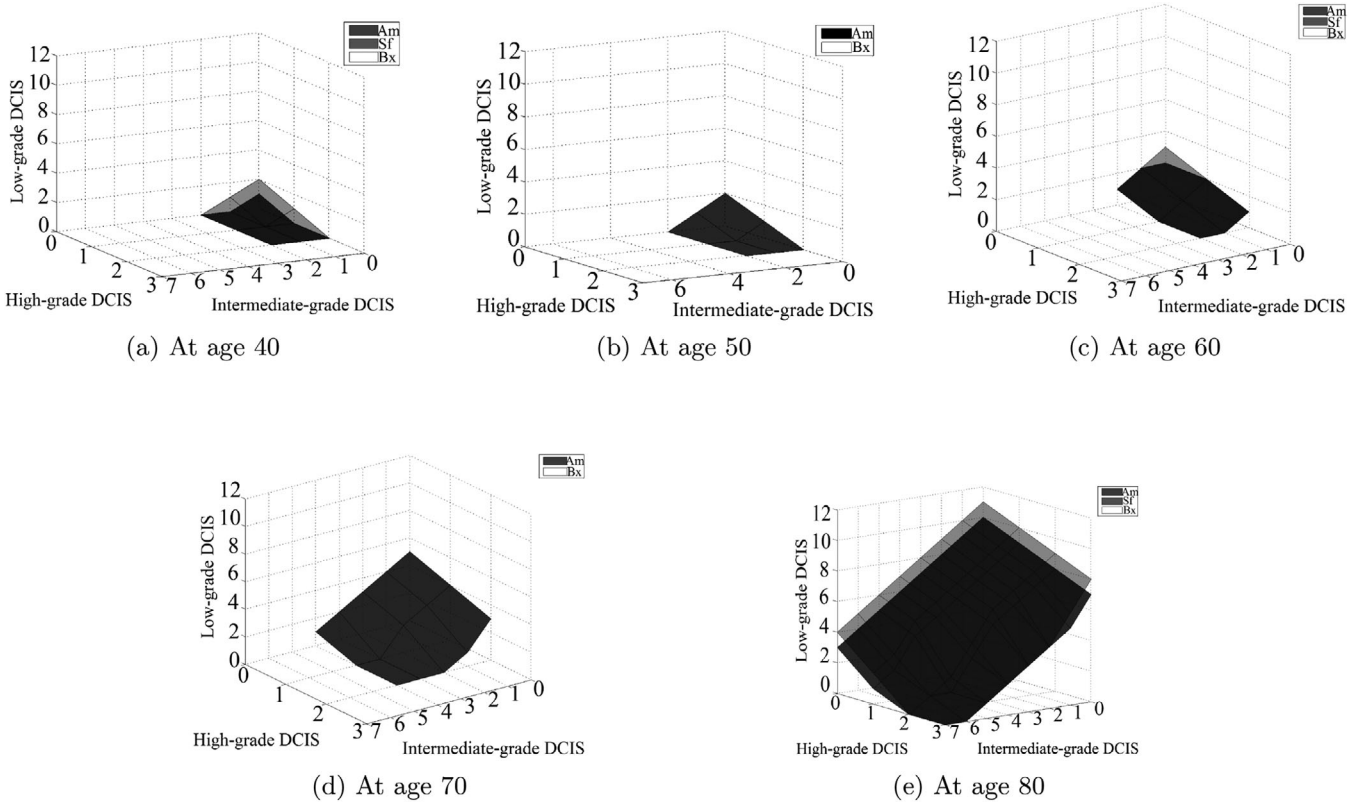

FIGURE 2 Optimal breast cancer diagnostic decisions when the probability of invasive cancer is 0%. For any state: below the black surface, the optimal action is Am; between the gray surface and the black surface, the optimal action is Sf; above the gray surface (white area), the optimal action is Bx

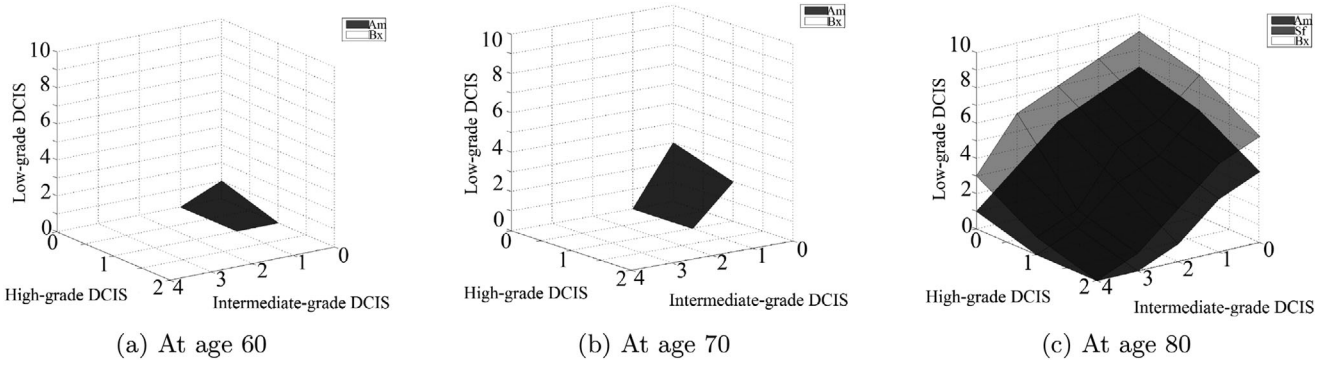

FIGURE 3 Optimal breast cancer diagnostic decisions when the probability of invasive cancer is 1%. For any state: below the black surface, the optimal action is Am; between the gray surface and the black surface, the optimal action is Sf; above the gray surface (white area), the optimal action is Bx

contribute to the alarming rates of overdiagnosis. To better assess the population-level impact of using the optimal guidelines from the LSM instead of the standard of care, we use the UWBCS simulation model to estimate the comparative effectiveness of the optimal policies in terms of the reduction in overdiagnosis, QALY gains, and the reduction in total costs related to screening, diagnosis, and treatment on the screening population.

Using the UWBCS model, we simulate women who were born in 1970 until all women from this birth cohort die. To comply with the LSM model assumptions, we consider the annual screening scenario with a 100% participation rate starting from age 40. Online Appendix B provides a more detailed discussion of the UWBCS model as well as the run settings used in our numerical experiment.

Table 1 demonstrates the population impact of the optimal diagnostic policies obtained by the LSM over the current practice in terms of the total QALY gain; the total decrease in cost, given by the total savings in the costs of surveillance mammography screening, diagnosis, and treatment; and the

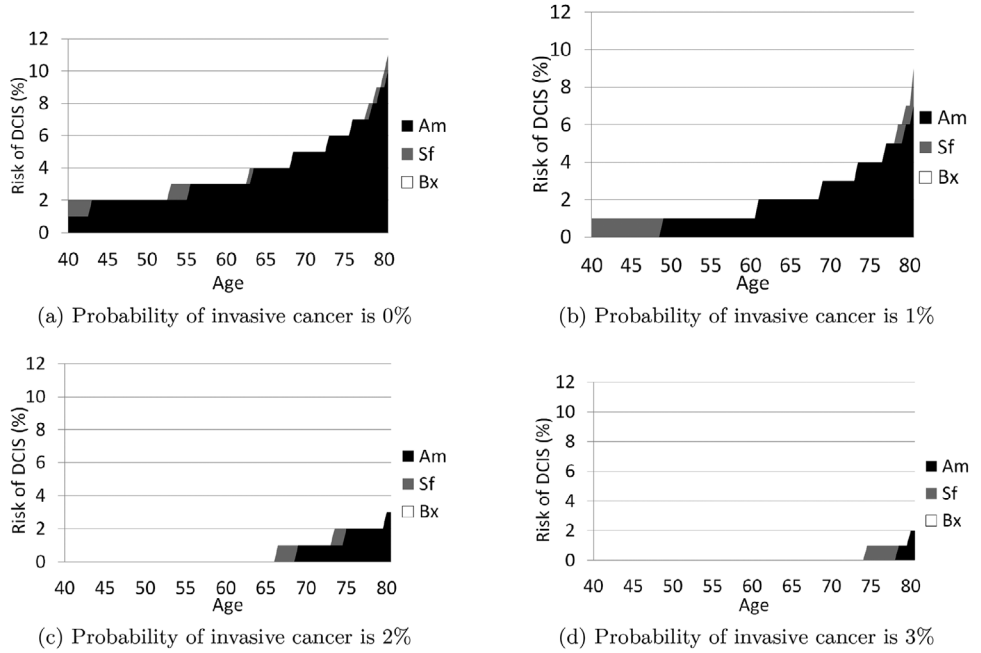

(a) Probability of invasive cancer is 0%

(b) Probability of invasive cancer is 1%

(c) Probability of invasive cancer is 2%

(d) Probability of invasive cancer is 3%

FIGURE 4 Age-specific optimal breast cancer diagnostic decisions as a function of aggregate DCIS risk for different levels of probability of invasive cancer

TABLE 1 Comparative effectiveness of the optimal breast cancer diagnosis

Age	QALY gain	Cost gain	Reduction in overdiagnosis (%)
40–54	7.1593	$23,777	**0.12**
55–59	18.9036	$367,084	**0.54**
60–64	110.5733	$1,397,448	**3.65**
65–69	197.4755	$4,319,253	**6.49**
70–74	288.6219	$8,158,207	**9.92**
75–79	348.7793	$11,056,208	**15.24**
>80	134.2853	$14,093,638	**15.53**
Total	**1105.7982**	**$39,415,616**	

Abbreviation: QALY, quality-adjusted life year.

FIGURE 5 Percentage of overdiagnosis averted using the optimal policy from the large-scale diagnostic decision model (LSM) [Color figure can be viewed at wileyonlinelibrary.com]

ratio of overdiagnosis averted for different age groups based on an initial population of 10 million women. Table 1 establishes that acknowledging the heterogeneity of cancer types, and accordingly, using the optimal personalized diagnosis in lieu of current clinical practice provides an overall 11.057 QALY and $394, 156 savings per 100,000 women. When projected on the U.S. population of women aged 40 and older, these numbers translate into 8310.86 QALY-gained across the population and over $296 million cost savings in the total breast cancer diagnostic expenses. Table 1 also confirms that a significant reduction in overdiagnosis can be obtained by replacing the current diagnostic practice with the optimal policy of the LSM, and highlights that the resulting QALY gains, cost savings, and overdiagnosis reduction become more prominent with increasing age.

To better illustrate the effect of age on the overdiagnosis reduction, Figure 5 presents the age-specific ratio of overdiagnosis averted by complying with the optimal policy instead of the current clinical guidelines. In Figure 5, the horizontal axis represents the age and the vertical axis represents the percentage of overdiagnosis averted. It shows that up to 20% reduction in overdiagnosis can be achieved when the optimal diagnostic policies replace the current biopsy threshold of 2%, which aggressively diagnose indolent breast cancer types such as the low-grade DCIS in older women, even though their life span may be lower than the sojourn time of the disease. Figure 5 emphasizes that the reduction in overdiagnosis steadily increases with age starting from age 60, which implies that older women, who bear the heaviest burden of overdiagnosis, benefit the most from the optimal

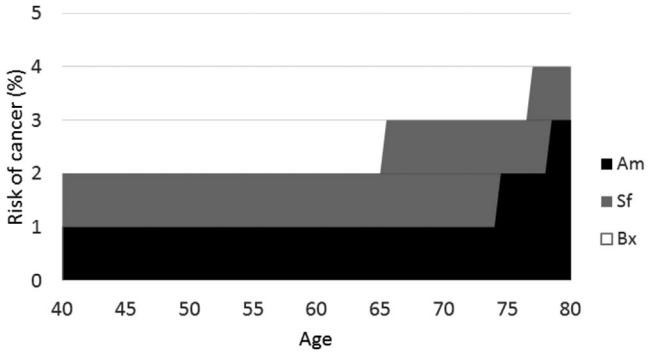

FIGURE 6 Age-specific optimal breast cancer diagnostic decisions from a conventional model

strategies obtained by the LSM in terms of the quality and span of life.

6.3 | Value of the large-scale MDP model

In this section, we estimate the value of solving a large-scale MDP model over solving a conventional lower dimensional optimization model. For this purpose, we compare the performance of the optimal policies from the LSM with that from a conventional MDP model employing a scalar probability of cancer that is typically used in the literature. We use our data sets to estimate the parameters of the conventional model including the transition probabilities, rewards, and disutilities instead of using the parameters from the literature to allow a more fair comparison between the large-scale model and the conventional one. Figure 6 presents the age-based optimal diagnostic policies obtained by the conventional MDP model as a function of scalar cancer risk. In Figure 6, the horizontal axis represents the age of the patient and the vertical axis represents the aggregate probability of cancer. Compared to Figure 4, Figure 6 shows that combining the risks of different DCIS grades and invasive cancer can lead to very aggressive biopsy recommendations, triggering the troubling practice of overdiagnosing low-risk diseases in the older population.

As an example from our clinical data, consider a 65-year-old woman with a heterogeneously dense breast and no family history of breast cancer having a mammogram that shows a cluster of amorphous, punctuate, and round calcifications. For this patient, our computer-aided diagnostic model predicts the risk vector as [96, 1, 2, 1, 0], and thus the optimal action recommended by the LSM is an annual mammogram. However, since the patient has a 4% probability of cancer, both the current clinical practice and the optimal policy obtained from the conventional model would recommend a biopsy, potentially leading to an overdiagnosis of highly indolent breast cancer in this aging woman.

To elucidate the effect of using our comprehensive model, which incorporates the discrepancy between the progression and death rates of cancer types, on overdiagnosis, Figure 7(a) provides the estimated age-based ratio of the biopsied population that would be overdiagnosed if a conventional model is used to optimize the diagnostic policies, instead of the LSM. Figure 7(a) illustrates that the conventional optimization approaches in the breast cancer diagnosis problem fail to address the issue of overdiagnosis, and a more comprehensive large-scale model such as the LSM that optimizes decisions by differentiating the risks of low-, intermediate-, high-grade DCIS, and invasive cancer is required for alleviating overdiagnosis of indolent diseases.

Figure 7(b) provides the estimated age-specific ratio of missed malignancies if the optimal policies of the LSM were used instead of those from a conventional model. When considered together with Figure 7(a), it demonstrates that up to 4% of biopsied population can be protected from being overdiagnosed only at the cost of missing 0–2 malignancies per 10,000 biopsied women using the large-scale optimization model.

We also evaluate the robustness of the LSM by performing a sensitivity analysis over the model parameters (see Figures 9 and 10 in Online Appendix D for details). We find that the biopsy thresholds become lower as the disutility of biopsy is reduced. Nevertheless, the LSM still outperforms the current clinical threshold of 2% and the conventional models in avoiding potentially unnecessary biopsies and concomitantly addressing overdiagnosis of low-risk diseases. Similarly, we observed that changing the disutilities of short-term follow-up and annual mammogram had a negligible effect on the performance of the LSM. Furthermore, the optimal diagnostic policy does not change significantly when we vary the DCIS progression rates within their 95% confidence intervals.

7 | CONCLUSION

In this paper, we optimize diagnostic decisions following a mammography screening based on mammographic findings and demographic factors, while considering the potential effects of these decisions on breast cancer overdiagnosis. By differentiating the risk of different breast cancer types, we develop a novel approach that improves the early diagnosis of invasive cancer while minimizing unnecessary diagnostic procedures such as biopsy on indolent findings. We formulate this diagnostic decision problem as a large-scale finite-horizon MDP to maximize the total QALYs of a patient. We develop efficient algorithms that utilize the structural properties of the optimal policy to find an exact optimal solution to the large-scale MDP instead of an approximate and suboptimal solution. Finally, we provide a dimension reduction method to formulate two alternative MDP models that are used to provide tight bounds on the optimal policy of the large-scale MDP, further improving the performance of our optimization algorithm.

The advancements in medical imaging technology and better prediction of disease types are creating an opportunity to make more personalized decisions in clinical management. However, optimization models for personalized diagnostic

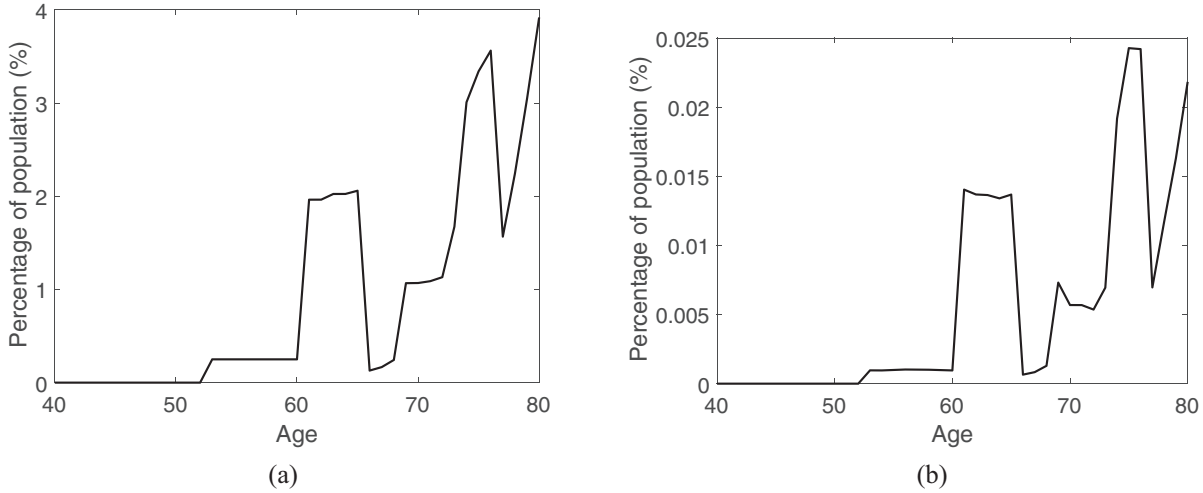

FIGURE 7 (a) Age-based percentage of the biopsied population who are saved from being overdiagnosed using the large-scale diagnostic decision model (LSM) as compared to the conventional model. (b) Age-specific percentage of the cancer cases that are missed using the LSM as compared to the conventional model

decisions are relatively sparse, while models specifying decisions for cancer types are nonexistent, to our knowledge. Our study constitutes a first step toward determining diagnostic guidelines specific to patients' age and cancer type. Our findings demonstrate the applicability of large-scale optimization models to the design of diagnostic policies aiming to decrease overdiagnosis. Our results demonstrate the importance of tailoring guidelines to patients' age and disease types. On one hand, our optimal policy agrees with the standard of care threshold for the younger population or when findings clearly indicate invasive cancer. On the other hand, the optimal policy recommends routine annual mammography for an older patient, who has a five times higher risk of low-grade DCIS than the standard of care risk threshold. These disparities help for the early diagnosis of invasive cancer while averting overdiagnosis of low-grade DCIS in aging women, for which the sojourn time of the disease may exceed their expected life span.

The application of our model to real-life mammography data from the UW and UCSF hospitals, and the simulation of our findings over a well-proven microsimulation model have yielded three main observations. First, our numerical results suggest that the use of optimal diagnostic guidelines elaborated by high-dimensional risk vectors in breast cancer decision making can substantially mitigate overdiagnosis in clinical practice. The comparative effectiveness analysis confirms that the optimal diagnosis of breast cancer based on disease type provides up to 20% reduction in overdiagnosis by offering less aggressive interventions for findings indicating indolent diseases. The optimal diagnosis of breast cancer is confirmed to be QALY-improving and cost-saving, providing an overall 11.057 additional QALY and $394,156 savings per 100,000 screened women when compared to current clinical practice. Second, our comprehensive approach provides significant benefits compared to lower dimensional conventional optimization models where a scalar probability is used to model the risk of cancer. Third, we observe that our approach has a more pronounced impact on older women compared to younger women. This further highlights the efficiency of our optimization model in reducing overdiagnosis as overdiagnosis of breast cancer may be more common and easier to detect in older women, who often have a limited life span due to other comorbidities.

Diagnosing indolent diseases, which leads to overdiagnosis and overtreatment if not recognized, is a problem whose scope reaches beyond breast cancer. A low-grade tumor of the prostate is a disease with probably the greatest risk for overdiagnosis (Esserman et al., 2014). Although these low-risk, less aggressive lesions are unlikely to cause symptoms or affect survival if left undiagnosed and untreated (Hoffman et al., 2014), most findings indicating low-risk lesions are followed with biopsy and 90% of the patients with a diagnosis of low-grade prostate cancer receive treatment (Cooperberg et al., 2010). Thyroid carcinoma is another example of how aggressive diagnosis and treatment of indolent lesions may lead to no health benefits (Cronan, 2008). Between 1975 and 2013, the incidence rate of thyroid cancer increased from 4.85 to 15.07 per 100,000, whereas death rates only slightly decreased from 0.55 to 0.52 per 100,000 in United States (Howlader et al., 2016). Overdiagnosis is a common problem even among cancers that are considered to have the highest growth rate and mortality, such as lung cancer (Welch & Black, 2010). A follow-up study of the Mayo Lung Project reveals that there is a 51% risk of overdiagnosis resulted from screen-detected cancers (Marcus et al., 2006). Our model provides a framework for future work to study various cancer diagnosis problems and help in reducing overdiagnosis by enabling the diagnostic thresholds specific to the disease types. Another important future research direction is to incorporate the optimal treatment plans of the diagnosed indolent diseases into the diagnostic decision framework to also help with the overtreatment issue.

In conclusion, our findings highlight a potential to address overdiagnosis with the help of a large-scale optimization model utilizing disease types. This adds a new dimension to the literature on cancer diagnostic decision making that has focused primarily on identifying optimal policies based on the probability of cancer ignoring the significant heterogeneity of various cancer types concerning their rate of progression and potential for leading to cancer death.

ACKNOWLEDGMENTS

We thank the Departmental Editor Sergei Savin, an anonymous senior editor, and two anonymous referees for their constructive suggestions that helped improve the paper. We thank Finn Kuusisto, Aparna Mahajan, Yirong Wu, and Jennifer Cox (University of Wisconsin-Madison) for their helpful feedback on the paper. This work was supported by National Cancer Institute Grants K24CA194251, R01CA165229, and P30CA014520 (University of Wisconsin Carbone Cancer Support Grant).

ENDNOTES

[1] We assume that the risk vectors are fully observable by the decision maker. A partially observable Markov decision process (POMDP) model may allow for including any observational error resulting from radiologists' assessment of mammography findings or implementation of computer-aided diagnostic models. However, any appropriate selection of an observation set to model postmammography decisions

(i) requires a very large amount of data to estimate the observation probabilities and

(ii) leads to a computationally intractable model that needs to be approximated by an MDP to be solved.

See Chhatwal et al. (2010) for an illustration of how even a simpler diagnostic POMDP model, which ignores types of cancer and short-term follow-up action, requires excessive data and computational effort, making the model unsuitable for the problem of choice.

[2] Notice that the probability of being cancer-free, $x^0 = 100 - \sum_{i=1}^{4} x^i$, is dropped from the state vector definition in $\mathcal{X}$. Although $\mathcal{X}$ and $\tilde{\mathcal{X}}$ are equivalent, we use the former in Section 4.1 because it provides a natural comparison of states, and the latter in Section 4.2 because it allows an intuitive projection into lower dimensions.

[3] Equivalently, we can say that it projects four-dimensional state space onto two-dimensional space since all state vectors are probability vectors.

REFERENCES

ACOG (2020). *ACOG mammography and other screening tests for breast problems*. https://www.acog.org/womens-health/faqs/mammography-and-other-screening-tests-for-breastproblems.

Alagoz, O., Berry, D. A., de Koning, H. J., Feuer, E. J., Lee, S. J., Plevritis, S. K., Schechter, C. B., Stout, N. K., Trentham-Dietz, A., & Mandelblatt, J. S. (2018a). Introduction to the Cancer Intervention and Surveillance Modeling Network (CISNET) breast cancer models. *Medical Decision Making*, *38*(1_suppl), 3S–8S.

Alagoz, O., Chhatwal, J., & Burnside, E. S. (2013). Optimal policies for reducing unnecessary follow-up mammography exams in breast cancer diagnosis. *Decision Analysis*, *10*(3), 200–224.

Alagoz, O., Ergun, M. A., Cevik, M., Sprague, B. L., Fryback, D. G., Gangnon, R. E., Hampton, J. M., Stout, N. K., & Trentham-Dietz, A. (2018b). The University of Wisconsin breast cancer epidemiology simulation model: An update. *Medical decision making*, *38*(1_suppl), 99S–111S.

Allred, D. C. (2010). Ductal carcinoma in situ: Terminology, classification, and natural history. *Journal of the National Cancer Institute Monographs*, *2010*(41), 134–138.

Arias, E. (2015). United States life tables, 2011. *National Vital Statistics Reports*, *64*(11), 1–62.

Arrospide, A., Rue, M., van Ravesteyn, N. T., Comas, M., Larrañaga, N., Sarriugarte, G., & Mar, J. (2015). Evaluation of health benefits and harms of the breast cancer screening programme in the Basque Country using discrete event simulation. *BMC Cancer*, *15*(1), 671.

Ayer, T., Alagoz, O., & Stout, N. K. (2012). OR forum—A POMDP approach to personalize mammography screening decisions. *Operations Research*, *60*(5), 1019–1034.

Ayer, T., Alagoz, O., Stout, N. K., & Burnside, E. S. (2015). Heterogeneity in women's adherence and its role in optimal breast cancer screening policies. *Management Science*, *62*(5), 1339–1362.

Ayvaci, M. U., Alagoz, O., & Burnside, E. S. (2012). The effect of budgetary restrictions on breast cancer diagnostic decisions. *Manufacturing & Service Operations Management*, *14*(4), 600–617.

Barlow, R., & Proschan, F. (1965). *Mathematical theory of reliability*. Wiley.

BI-RADS (2003). *Breast imaging reporting and data system* (*BI-RADS*), 4th ed. American College of Radiology.

Bleyer, A., & Welch, H. G. (2012). Effect of three decades of screening mammography on breast-cancer incidence. *New England Journal of Medicine*, *367*(21), 1998–2005.

Cevik, M., Ayer, T., Alagoz, O., & Sprague, B. L. (2018). Analysis of mammography screening policies under resource constraints. *Production and Operations Management*, *27*(5), 949–972.

Chhatwal, J., Alagoz, O., & Burnside, E. S. (2010). Optimal breast biopsy decision-making based on mammographic features and demographic factors. *Operations Research*, *58*(6), 1577–1591.

CNN (2018). *Too many medical tests may harm, not help, older patients*. https://www.cnn.com/2018/01/03/health/medical-screening-older-patients-partner/index.html.

Cooperberg, M. R., Broering, J. M., & Carroll, P. R. (2010). Time trends and local variation in primary treatment of localized prostate cancer. *Journal of Clinical Oncology*, *28*(7), 1117–1123.

Cronan, J. J. (2008). Thyroid nodules: Is it time to turn off the US machines? *Radiology*, *247*(3), 602–604.

Davidov, O., & Zelen, M. (2004). Overdiagnosis in early detection programs. *Biostatistics*, *5*(4), 603–613.

Drummond, M. F., Sculpher, M. J., Claxton, K., Stoddart, G. L., & Torrance, G. W. (2015). *Methods for the economic evaluation of health care programmes*. Oxford University Press.

Duffy, S. W., Agbaje, O., Tabar, L., Vitak, B., Bjurstam, N., Björneld, L., Myles, J. P., & Warwick, J. (2005). Overdiagnosis and overtreatment of breast cancer: Estimates of overdiagnosis from two trials of mammographic screening for breast cancer. *Breast Cancer Research*, *7*(6), 258–265.

Eckles, J. E. (1968). Optimum maintenance with incomplete information. *Operations Research*, *16*(5), 1058–1067.

Esserman, L. J., Thompson, I. M., & Reid, B. (2013). Overdiagnosis and overtreatment in cancer: An opportunity for improvement. *JAMA*, *310*(8), 797–798.

Esserman, L. J., Thompson, I. M., Reid, B., Nelson, P., Ransohoff, D. F., Welch, H. G., Hwang, S., Berry, D. A., Kinzler, K. W., Black, W. C., Bissell, M., Parnes, H. & Srivastava, S. (2014). Addressing overdiagnosis and overtreatment in cancer: A prescription for change. *The Lancet Oncology*, *15*(6), e234–e242.

Esserman, L. J., Yau, C., Thompson, C. K., Van't Veer, L. J., Borowsky, A. D., Hoadley, K. A., Tobin, N. P., Nordenskjöld, B., Fornander, T., Stål, O., Benz, C. C., & Lindström, L. S. (2017). Use of molecular tools to identify patients with indolent breast cancers with ultralow risk over 2 decades. *JAMA Oncology*, *3*(11), 1503–1510.

Fisher, B., Land, S., Mamounas, E., Dignam, J., Fisher, E. R., & Wolmark, N. (2001). Prevention of invasive breast cancer in women with ductal carcinoma in situ: An update of the national surgical adjuvant breast and bowel project experience. *Seminars in Oncology*, *28*(4), 400–418.

Gunsoy, N., Garcia-Closas, M., & Moss, S. (2014). Estimating breast cancer mortality reduction and overdiagnosis due to screening for different trategies in the United Kingdom. *British Journal of Cancer*, *110*(10), 2412–2419.

Helm, J. E., Lavieri, M. S., Van Oyen, M. P., Stein, J. D., & Musch, D. C. (2015). Dynamic forecasting and control algorithms of glaucoma progression for clinician decision support. *Operations Research*, *63*(5), 979–999.

Hoffman, K. E., Niu, J., Shen, Y., Jiang, J., Davis, J. W., Kim, J., Kuban, D. A., Perkins, G. H., Shah, J. B., Smith, G. L., Volk, R. J., Buchholz, T. A., Giordano, S. H., & Smith, B. D. (2014). Physician variation in management of low-risk prostate cancer: A population-based cohort study. *JAMA Internal Medicine*, *174*(9), 1450–1459.

Howlader, N., Noone, A., Krapcho, M., Miller, D., Bishop, K., Altekruse, S., Kosary, C., Yu, M., Ruhl, J., Tatalovich, Z., Mariotto, A., Lewis, D., Chen, H., Feuer, E., & Cronin, K. (2016). *SEER cancer statistics review,* 1975-2013. National Cancer Institute. Bethesda, MD.

Irshad, S., Bansal, M., Castillo-Martin, M., Zheng, T., Aytes, A., Wenske, S., Le Magnen, C., Guarnieri, P., Sumazin, P., Benson, M. C., Shen, M. M., Califano, A., & Abate-Shen, C. (2013). A molecular signature predictive of indolent prostate cancer. *Science Translational Medicine*, *5*, 202ra122.

Jørgensen, K. J., Gøtzsche, P. C., Kalager, M., & Zahl, P.-H. (2017). Breast cancer screening in Denmark: A cohort study of tumor size and overdiagnosis. *Annals of Internal Medicine*, *166*(5), 313–323.

Khatib, O. M., & Modjtabai, A. (2006). *Guidelines for the early detection and screening of breast cancer*. World Health Organization, Regional Office for the Eastern Mediterranean.

Kuusisto, F. C. (2015). *Machine learning for medical decision support and individualized treatment assignment*. [Ph.D. thesis, University of Wisconsin-Madison].

Madadi, M., Heydari, M., Zhang, S., Pohl, E., Rainwater, C., & Williams, D. L. (2018). Analyzing overdiagnosis risk in cancer screening: A case of screening mammography for breast cancer. *IISE Transactions on Healthcare Systems Engineering*, *8*(1), 2–20.

Maillart, L. M., Ivy, J. S., Ransom, S., & Diehl, K. (2008). Assessing dynamic breast cancer screening policies. *Operations Research*, *56*(6), 1411–1427.

Makis, V. (2008). Multivariate Bayesian control chart. *Operations Research*, *56*(2), 487–496.

Marcus, P. M., Bergstralh, E. J., Zweig, M. H., Harris, A., Offord, K. P., & Fontana, R. S. (2006). Extended lung cancer incidence follow-up in the Mayo Lung Project and overdiagnosis. *Journal of the National Cancer Institute*, *98*(11), 748–756.

Medscape (2020). *"Overdiagnosis" in about* 20% *of common cancers*. https://www.medscape.com/viewarticle/924550.

Miller, A. B., Wall, C., Baines, C. J., Sun, P., To, T., & Narod, S. A. (2014). Twenty five year follow-up for breast cancer incidence and mortality of the Canadian National Breast Screening Study: Randomised screening trial. *BMJ*, *348*, g366.

New York Times (2017). *Too many older patients get cancer screenings*. https://www.nytimes.com/2017/12/19/well/live/cancer-screening-tests-seniors-older-patients-harms-overdiagnosis-overtreatment.html.

Ong, M.-S., & Mandl, K. D. (2015). National expenditure for false-positive mammograms and breast cancer overdiagnoses estimated at 4 billion a year. *Health Affairs*, *34*(4), 576–583.

Paç, M. F., & Veeraraghavan, S. (2015). *False diagnosis and overtreatment in services*. Tech. rep., Working paper, University of Pennsylvania, Philadelphia.

Puterman, M. L. (1994). *Markov decision processes: Discrete stochastic dynamic programming*. John Wiley & Sons

Seigneurin, A., François, O., Labarère, J., Oudeville, P., Monlong, J., & Colonna, M. (2011). Overdiagnosis from non-progressive cancer detected by screening mammography: Stochastic simulation study with calibration to population based registry data. *BMJ*, *343*, d7017.

Siegel, R. L., Miller, K. D., & Jemal, A. (2015). Cancer statistics, 2015. *CA: A Cancer Journal For Clinicians*, *65*(1), 5–29.

Srivastava, S., Koay, E. J., Borowsky, A. D., De Marzo, A. M., Ghosh, S., Wagner, P. D., & Kramer, B. S. (2019). Cancer overdiagnosis: A biological challenge and clinical dilemma. *Nature Reviews Cancer*, *19*(6), 349–358.

van Luijt, P., Heijnsdijk, E., Fracheboud, J., Overbeek, L., Broeders, M., Wesseling, J., den Heeten, G., & de Koning, H. (2016). The distribution of ductal carcinoma in situ (DCIS) grade in 4232 women and its impact on overdiagnosis in breast cancer screening. *Breast Cancer Research*, *18*(1), 47.

Virnig, B. A., Shamliyan, T., Tuttle, T. M., Kane, R. L., & Wilt, T. J. (2009). Diagnosis and management of ductal carcinoma in situ (DCIS). *Evidence Report/Technology Assessment*, *185*, 1–549.

Washington Post (2017). *Doing more harm than good? Epidemic of screening burdens nation's older patients*. https://www.washingtonpost.com/national/health-science/doing-more-harm-than-good-epidemic-of-screening-burdens-nations-older-patients/2017/12/20/b46d0564-e56e-11e7-927a-e72eac1e73b6_story.html.

Welch, H. G., & Black, W. C. (2010). Overdiagnosis in cancer. *Journal of the National Cancer Institute*, *102*(9), 605–613.

SUPPORTING INFORMATION

Additional supporting information may be found in the online version of the article at the publisher's website.

How to cite this article: Tunç, S., Alagoz, O., & Burnside, E. S. (2022). A new perspective on breast cancer diagnostic guidelines to reduce overdiagnosis. *Production and Operations Management*, 31, 2361–2378. https://doi.org/10.1111/poms.13691